Materials Research. 2023; 26: e20220371
DOI: https://doi.org/10.1590/1980-5373-MR-2022-0371

First-Principles Comparative Study of $CuFeSe_2$ and $CuFeS_2$

Xiaofan Liu[a], Jie Du[a], Long Hua[a], Kegao Liu[a]*

[a]*Shandong Jianzhu University, School of Materials Science and Engineering, Fengming Road 1000, Jinan 250101, China.*

Received: August 18, 2022; Revised: November 02, 2022; Accepted: December 15, 2022

In this paper, on the basis of first-principles, the CASTEP module of Materials Studio is used to calculate the band structures and optical properties of $CuFeSe_2$ and $CuFeS_2$ under the PBE pseudopotential of the generalized gradient approximation (GGA). The calculated results show that both $CuFeSe_2$ and $CuFeS_2$ are direct bandgap semiconductors with forbidden band widths of 0.64 eV and 1.06 eV, respectively. In the visible light range, the highest absorption coefficient of $CuFeSe_2$ is 1.082×10^5 cm^{-1}, the average reflectivity is 0.52, the maximum conductivity is 7.23 fs^{-1}, the electrostatic constant is 65.9; the maximum value the highest absorption coefficient of $CuFeS_2$ is 0.872×10^5 cm^{-1}, the average reflectivity is 0.44, the maximum conductivity is 4.44 fs^{-1}, the static dielectric constant is 52.32. The calculation results in this paper show that compared with $CuFeS_2$, $CuFeSe_2$ has advantages in photoconductivity and carrier separation, but has disadvantages in band gap and reflectivity. It is recommended to combine the two materials to prepare tandem solar cells.

Keyword: *First-principles calculation, energy band, optical property, $CuFeSe_2$, $CuFeS_2$.*

1. Introduction

In recent years, the consumption of energy has been increasing day by day, and traditional fossil energy, as a non-renewable resource, cannot support the sustainable development for human beings. Therefore, the utilization of renewable energy has become the general trend. Among them, solar photovoltaic power generation relies on its abundant resources, cleanliness and pollution-free, etc. It has become one of the most potential renewable energy sources[1]. Traditional solar photovoltaic cells are made of crystalline silicon and utilize p-n junctions in the silicon material to achieve carrier separation and output. However, crystalline silicon solar cells consume large raw materials, complex processes, high power consumption and high cost in the production process, and it is difficult to further improve the photoelectric conversion rate. Therefore, researchers began to study thin-film solar cells with simpler manufacturing methods, less energy consumption, and higher photoelectric conversion efficiency[2,3].

Copper indium selenide and copper indium gallium selenide (Cu-In-Ga-Se, CIGS) thin-film solar cells have become research hot spots because of their high visible light absorption coefficient, stable performance, and long service life[4-6]. However, as one of the raw materials, indium is scarce, expensive and toxic[7]. Therefore, the search for new cheap and non-toxic alternative materials has become a research hot spot. As a typical chalcopyrite structure semiconductor material[8], $CuFeS_2$ is a direct bandgap semiconductor[9], with high light absorption coefficient[10], good thermal stability, no light-induced recession effect, and abundant raw material reserves, low cost, non-toxic and harmless[11], it has the potential as a thin-film solar Absorbent layer material. However, the low conductivity of $CuFeS_2$ limits its photovoltaic performance. Replacing sulfur with selenium is a common modification method for sulfide semiconductor materials. The literature shows that most of the chalcogen compounds show such a law: when the oxygen in the oxide is replaced by sulfur, or the sulfur is replaced by selenium, the forbidden band width of the material usually becomes smaller, and the electrical conductivity usually becomes larger[12]. However, this law lacks systematic and theoretical research, and cannot be directly applied to $CuFeS_2$ materials. In order to explore the difference between the properties of $CuFeSe_2$ and $CuFeS_2$, to find a more suitable material for the solar energy absorption layer than $CuFeS_2$, this paper uses first-principles calculations to compare the energy band structure, light absorptivity and reflectivity, photoconductivity, dielectric function. The properties of $CuFeSe_2$ and $CuFeS_2$ were analyzed, and their advantages and disadvantages as absorbent layer materials for solar cells were systematically evaluated. The structure and advantages and disadvantages of the four solar cells are shown in Figure 1[13-15].

2. Calculation Method

According to many literatures[16,17] and the results further confirmed in the ICSD database and Findit software in this paper, the models of $CuFeSe_2$ and $CuFeS_2$ are shown in Figure 2. $CuFeS_2$ belongs to the I-42d space group 122[17]. $CuFeSe_2$ belongs to the P-42C space group 112, and this structure can be regarded as a sulfovanadate derivative structure rather than the chalcopyrite-type structure expected for typical I-III-VII semiconductor compounds[18,19]. Both systems were calculated using first-principles calculations

*e-mail: liukg163@163.com

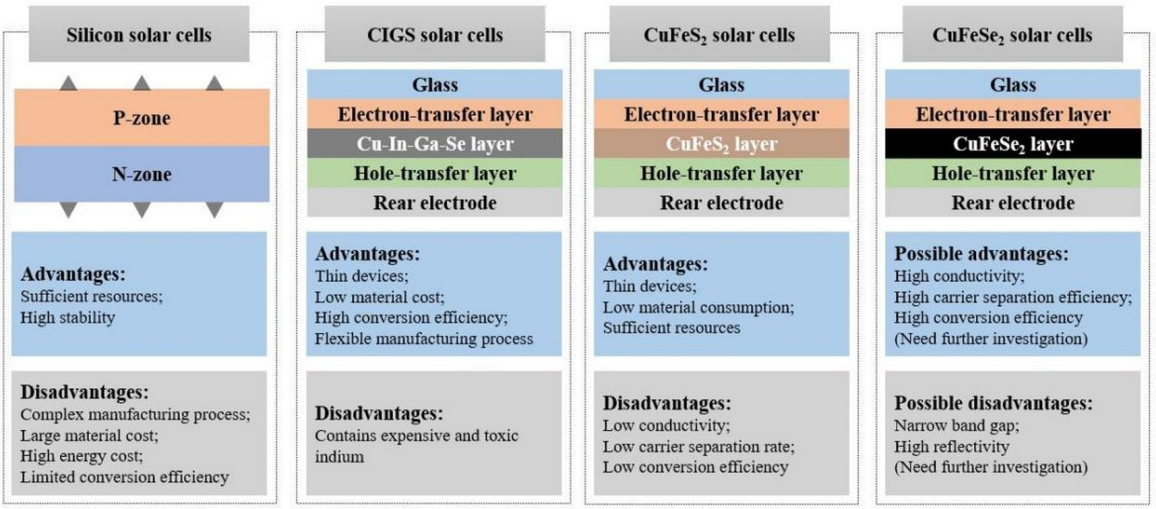

Figure 1. Schematic diagram of the structure of crystalline silicon, CIGS, $CuFeS_2$ cells and $CuFeSe_2$ solar cells and the comparison of possible advantages and disadvantages.

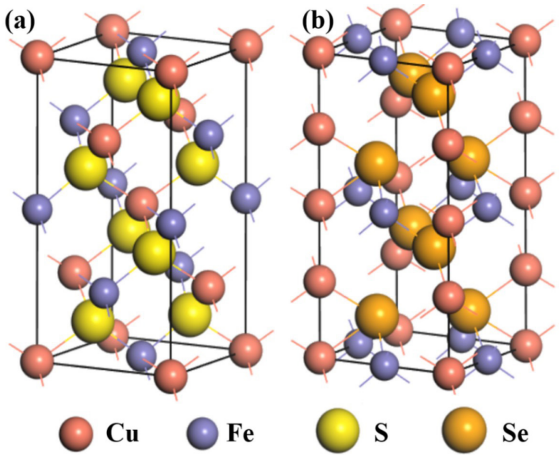

Figure 2. Schematic diagrams of crystal models of (a) $CuFeS_2$ and (b) $CuFeSe_2$.

based on density functional theory (DFT)[20,21]. Using the Cambridge Sequential Total Energy Package (CASTEP) module of Materials Studio, the generalized gradient approximation (GGA) and PBE pseudopotentials are used to complete the calculation[22]. The calculation content includes structure optimization, energy band calculation, density of states and optical properties (including light absorption rate, reflectivity, photoconductivity, dielectric function). The plane wave cutoff energy of both systems is set to 440.0 eV, and the k-point density of the Brillouin zone is set to 4×4×2.

3. Calculation Results and Analysis

3.1. Model construction and structure optimization of $CuFeSe_2$ and $CuFeS_2$

The optimization results of $CuFeSe_2$ and $CuFeS_2$ are shown in Table 1. The table data shows that the lattice constants a, b, c and the unit cell volume of $CuFeSe_2$ are all larger than those of $CuFeS_2$. After the structure optimization, the lattice constants a, b, c and the unit cell volume of the two crystals are smaller than those before optimization.

Table 1. Lattice constants and unit cell volumes of $CuFeSe_2$ and $CuFeS_2$ before and after optimization.

Chemical composition		$CuFeS_2$	$CuFeSe_2$
Lattice constant a, b(Å)	Before optimization	5.2890	5.5300
	After optimization	5.1270	5.2543
Lattice constant c(Å)	Before optimization	10.4230	11.0490
	After optimization	10.0211	10.6281
Cell volume V(Å^3)	Before optimization	291.5680	337.8880
	After optimization	263.4190	293.4180

3.2. Energy band calculation and density of states calculation of $CuFeSe_2$ and $CuFeS_2$

Figure 3a and 3b shows the energy band and density of states of $CuFeSe_2$. The forbidden band width of $CuFeSe_2$ is 0.64 eV, and it is a straight-gap semiconductor, which is larger than that measured in the literature (~0.4 eV). The main reason for this error is that the model used in the theoretical calculation is a perfect intrinsic semiconductor with no impurities and no lattice defects. The actual $CuFeSe_2$ crystal has various defects, which makes the actual energy band width lower than the theoretical value. Figure 3c and 3d shows the energy band and density of states of $CuFeS_2$. $CuFeS_2$ is also a straight-gap semiconductor with a band gap of 1.06 eV, which is also slightly larger than the measured band gap (~0.7 eV). It can be seen from Figure 3b and 3d that the slope of conduction band edge of $CuFeSe_2$ is smaller than that of $CuFeS_2$, indicating that $CuFeSe_2$ has strong electron localization and is easily excited by external energy to become free electrons, which is conducive to its photoelectric conversion efficiency as the absorption layer of solar cells.

Figure 4a is the partial wave density of states map of $CuFeSe_2$. It can be seen from the figure that the electron density of $CuFeSe_2$ in the -17.0 eV to -14.5 eV region is

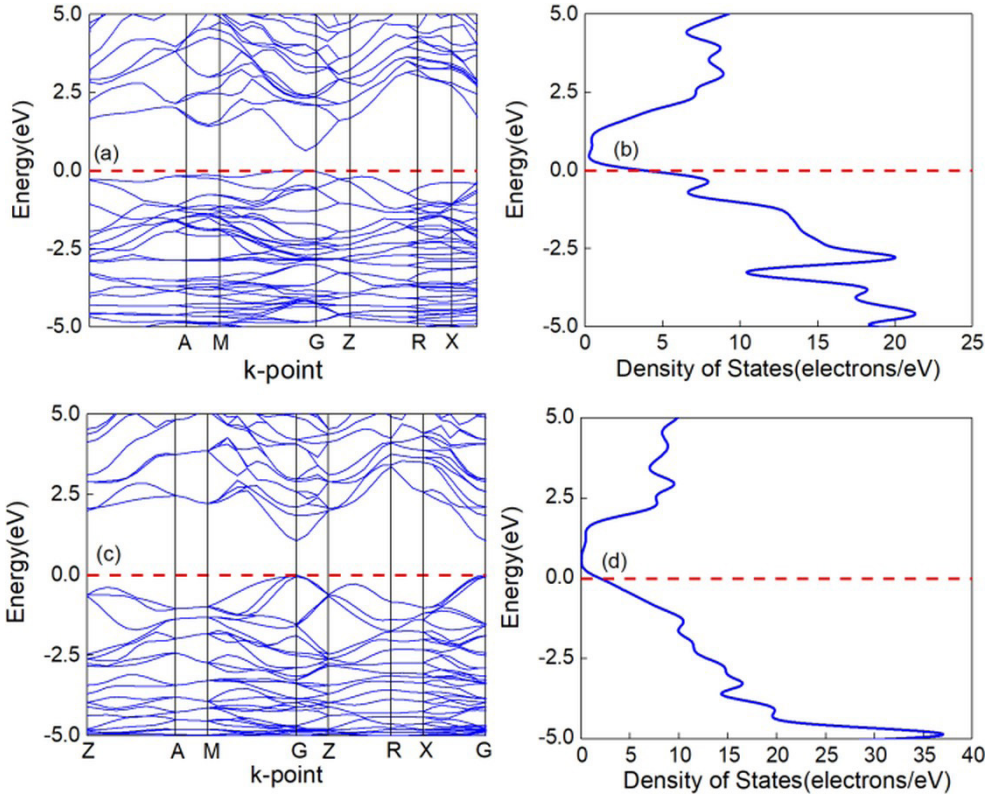

Figure 3. (a) (b) Energy band diagram and density diagram of states of $CuFeSe_2$; (c)(d) Energy band diagram and density diagram of states of $CuFeS_2$.

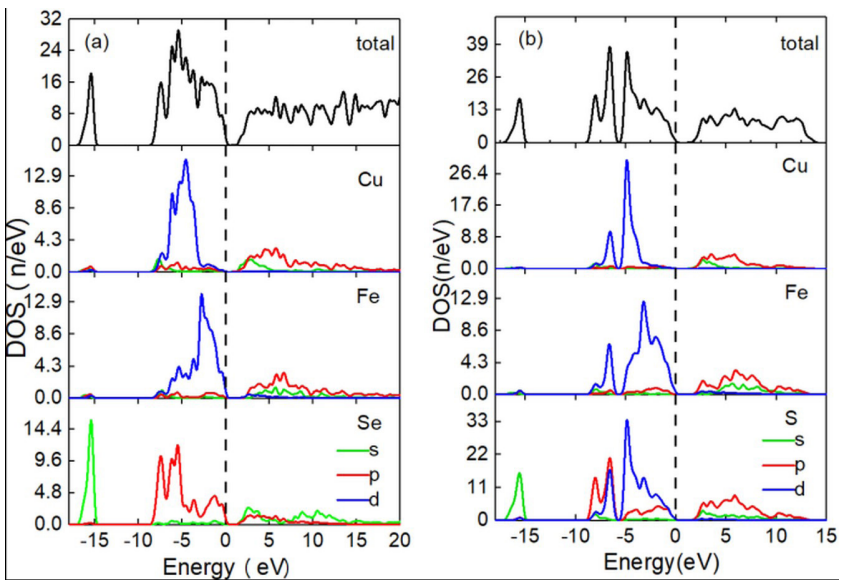

Figure 4. (a) Fractional density of states of $CuFeSe_2$, (b) Fractional density of states of $CuFeS_2$.

mainly contributed by the s electrons of Se, and mainly consists of the d state of Cu and the p state of Se in the range of -9.0 eV to -3.2 eV. The electronic density of states in the -3.2 eV to 0 eV region is mainly composed of d-state electrons of Fe and p-state electrons of Se. The conduction band region of $CuFeSe_2$ is mainly composed of the p-state electrons of Cu, Fe, and Se and the s-state electrons of Se, and the s-state electrons of Cu and Fe also have a small contribution.

The fractional density of states map of $CuFeS_2$ in Figure 4b shows that the electron density from -17.0 eV to -14.0 eV is mainly composed of the s states of the S element. The d electrons of Cu, Fe, S and the p electrons of S are the main constituents of -9.0 eV to 0 eV. The electron density of the

conduction band of $CuFeS_2$ is mainly composed of the p states of Cu, Fe, and S, and the s states of these three also contribute to a certain extent.

3.3. Calculation of optical properties of $CuFeSe_2$ and $CuFeS_2$

3.3.1. Absorptivity and reflectivity of $CuFeSe_2$ and $CuFeS_2$

Absorption rate is the ratio of the solar energy absorbed by a material over the full range of wavelengths of sunlight to the total solar energy that reaches the surface of the material. Figure 5a presents the absorptivity map of $CuFeSe_2$ and $CuFeS_2$.It can be seen from Figure 5a that in the visible light range, the average absorption coefficient of $CuFeSe_2$ is 0.911×105 cm^{-1}, and the highest absorption coefficient is 1.082×10^5 cm^{-1}. In the visible light range (1.6~3.2 eV), the average absorption coefficient of $CuFeS_2$ is 0.858×10^5 cm^{-1}, and the maximum value is 0.872×10^5 cm^{-1}. Reflectance is the ratio of the amount of solar energy reflected by a material over the full range of wavelengths of the sun's rays to the total amount of solar energy reaching the material's surface. Figure 5b shows the reflectivity of $CuFeSe_2$ and $CuFeS_2$. In the visible light range, the average reflectance of $CuFeSe_2$ is 0.52, and the average reflectance of $CuFeS_2$ is 0.44. In contrast, in the visible light range, $CuFeSe_2$ has better light absorption properties than $CuFeS_2$. But $CuFeSe_2$ is also more reflective in the visible range. Considering that the anti-reflection film of the solar cell can effectively reduce the reflected light on the surface of the cell, although the reflectivity of $CuFeSe_2$ is slightly higher, its adverse effect as the absorption layer of the solar cell can be eliminated. Comparing the absorptivity diagrams of the two substances, it can be found that the absorption coefficient of $CuFeSe_2$ is high in the visible light range, and the absorption peak of $CuFeS_2$ is blue-shifted.

3.3.2. Calculation of photoconductivity of $CuFeSe_2$ and $CuFeS_2$

Photoconductivity determines the electrical conductivity of optoelectronic materials under illumination, and has a direct impact on the performance of solar cell materials. Light absorption makes the semiconductor form non-equilibrium carriers, and the increase of carrier concentration must increase the conductivity of the sample. This phenomenon of increasing the conductivity of the semiconductor caused by light is called photoconductance effect, and the corresponding conductivity is called photoconductivity. Figure 6a and 6b are the real and imaginary parts of the theoretically calculated photoconductivity of $CuFeSe_2$ and $CuFeS_2$, respectively. In the visible light range, the photoconductivity of $CuFeSe_2$ is significantly higher than

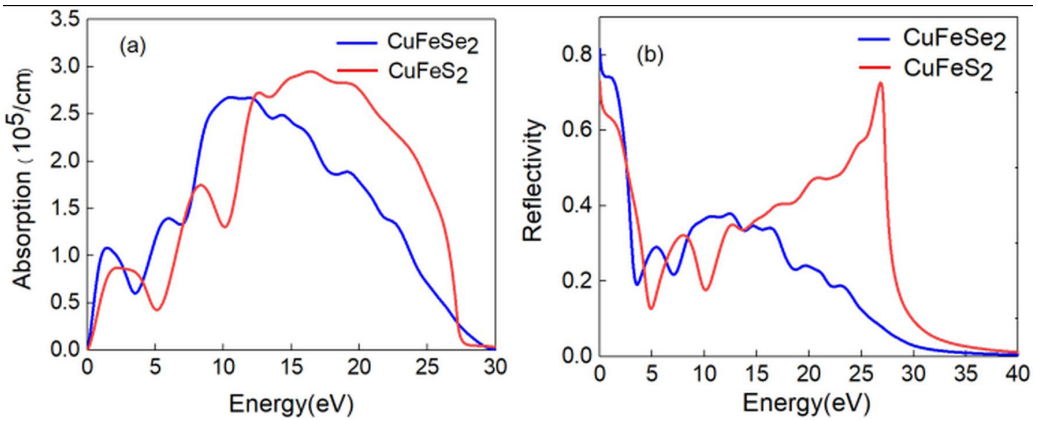

Figure 5. (a) Absorptivity and (b) Reflectance of $CuFeSe_2$ and $CuFeS_2$.

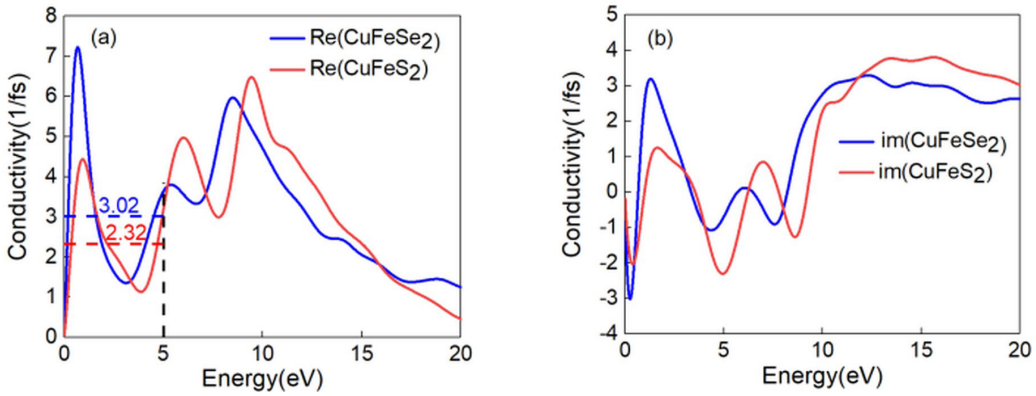

Figure 6. (a) real part and (b) imaginary part of photoconductivity of $CuFeSe_2$ and $CuFeS_2$.

that of $CuFeS_2$. The photoconductivity of $CuFeSe_2$ reaches the maximum value of 7.23 fs^{-1} at the incident photon energy of 0.689 eV, and the average photoconductivity is 3.02 fs^{-1}. The $CuFeS_2$ photoconductivity peaks at 4.44 fs^{-1} at 0.926 eV, and the average photoconductivity is 2.32 fs^{-1}. The photoconductivity of $CuFeSe_2$ is about 30% higher than that of $CuFeS_2$, and it is more suitable as an absorbent layer material for solar cells.

In this paper, the electron density of $CuFeS_2$ and $CuFeSe_2$ is simulated, and the physical models are constructed to explain the photoconductivity of them.As can be seen from the Figure 7, the volume of electron cloud overlapping between atoms in $CuFeSe_2$ crystal is larger, which is conducive to electron transfer, and thus its electrical conductivity is higher, making $CuFeSe_2$ a potential material for solar cell absorption layer.

3.3.3. Complex dielectric functions of $CuFeSe_2$ and $CuFeS_2$

The dielectric function is a bridge connecting the microphysical process of the interband transition and the electronic structure of the solid, which reflects the band structure of the solid and various other kinds of spectral information. In the linear response range, the solid macroscopic optical response function is described by the complex dielectric function[23]. The complex dielectric function $\varepsilon(\omega)$ consists of a real part $\varepsilon_1(\omega)$ and an imaginary part $\varepsilon_2(\omega)$. The real part of the dielectric function represents the ability of the dielectric to bind charges under the action of an external electric field, and the imaginary part can reflect the transition process of electrons between energy bands[24,25]. The formula is as follows:

$$\varepsilon(\omega) = \varepsilon_1(\omega) + i\varepsilon_2(\omega) \quad (1)$$

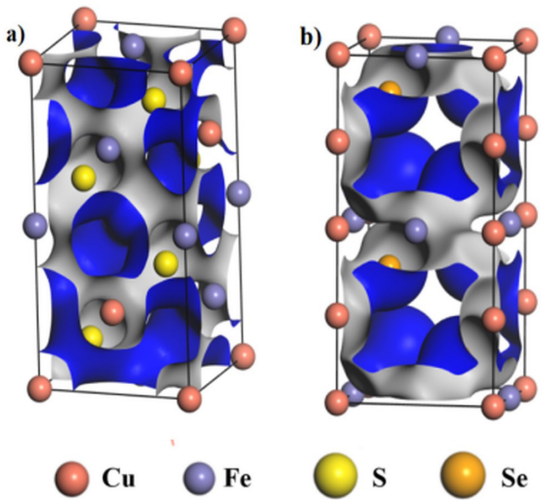

Figure 7. a) Electron density of $CuFeS_2$ and b) Electron density of $CuFeSe_2$.

Both $CuFeSe_2$ and $CuFeS_2$ are direct band gap semiconductor materials, and their spectra are generated by electronic transitions between energy levels, and each dielectric peak can be explained by the energy band structure and density of states. Figure 8 is a graph of the theoretically calculated complex permittivity function of $CuFeSe_2$ and $CuFeS_2$ as a function of photon energy. When there is no incident light, it corresponds to the static permittivity. Permittivity is a physical quantity that describes a material put into a capacitor to increase its ability to store charge. The electrostatic permittivity of $CuFeSe_2$ is 65.9 and that of $CuFeS_2$ is 52.3, indicating that the $CuFeSe_2$ system has a higher photogenerated electric field intensity and higher carrier separation efficiency, laying the foundation for high-efficiency solar power generation. The imaginary parts of the dielectric functions of $CuFeSe_2$ and $CuFeS_2$ increase sharply in the range of 0-6 eV, and each has a main peak. The secondary peaks of $CuFeSe_2$ at 7.3 eV and 10.3 eV, and the secondary peaks of $CuFeS_2$ at 6.9 eV and 10.4 eV, respectively, are caused by electronic transitions, which can be analyzed from the density of states diagram[25].

4. Conclusion

In this paper, first-principles calculations are performed on the band structures and optical properties of $CuFeSe_2$ and $CuFeS_2$. The calculation results show that $CuFeSe_2$ has two disadvantages as a light-absorbing layer for solar cells: the band gap of 0.64 eV is smaller than that of $CuFeS_2$, which is 1.06 eV, and the reflectivity in the visible light range is larger than that of $CuFeS_2$. However, $CuFeSe_2$ has unique

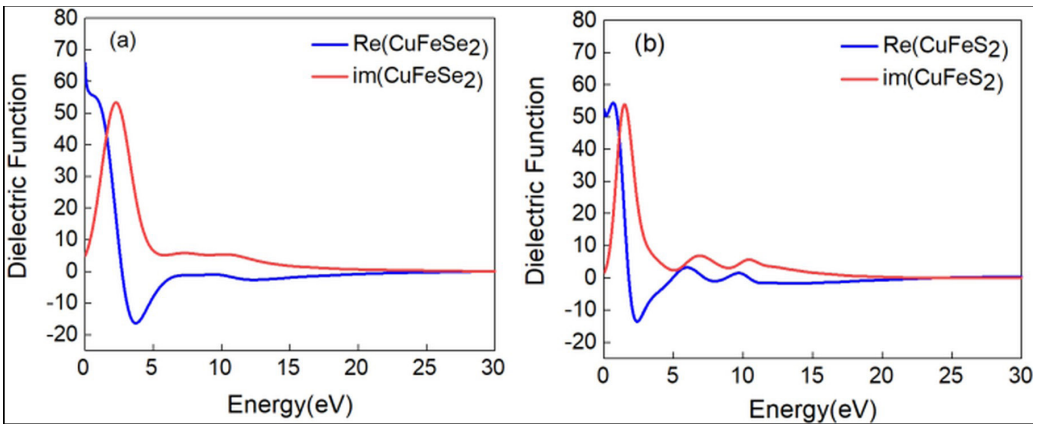

Figure 8. The real and imaginary parts of the complex dielectric functions of (a) $CuFeSe_2$ and (b) $CuFeS_2$.

advantages. In the visible light range, $CuFeSe_2$ has higher absorption rate and higher electrical conductivity, which is beneficial to its performance as an absorption layered material for solar cells.

From what has been said, a conclusion is drawn. Due to its narrow band gap and high reflectivity, $CuFeSe_2$ is not suitable for use as a light-absorbing layer material alone, and the stacking with $CuFeS_2$ happens to make up for the defects of $CuFeSe_2$. It is recommended to use the two in combination to form a $CuFeS_2$/$CuFeSe_2$ stacked battery, using $CuFeS_2$ as a wide-bandgap absorption layer and anti-reflection layer, $CuFeSe_2$ acts as a narrow bandgap absorption layer to achieve full utilization of solar radiation.

5. Acknowledgments

This work was financially supported by the National Natural Science Foundation of China (No.51272140).

6. References

1. Hosenuzzaman M, Rahim NA, Selvaraj J, Hasanuzzaman M, Malek A, Nahar A. Global prospects, progress, policies, and environmental impact of solar photovoltaic power generation. Renew Sustain Energy Rev. 2015;41:284-97.
2. Wang H. Progress in thin film solar cells based on Cu_2ZnSnS_4. Int J Photoenergy. 2011;2011(11):1683-91.
3. Ishizaki K, De Zoysa M, Tanaka Y, Jeon S-W, Noda S. Progress in thin-film silicon solar cells based on photonic-crystal structures. Jpn J Appl Phys. 2018;57(6):060101.
4. Stolt L, Hedstrom J, Kessler J, Ruckh M, Velthaus K-O, Schock H-W. Zno/Cds/$Cuinse_2$ thin-film solar-cells with improved performance. Appl Phys Lett. 1993;62(6):597-9.
5. Wada T. $CuInSe_2$ and related I–III–VI_2 chalcopyrite compounds for photovoltaic application. Jpn J Appl Phys. 2021;60(8):080101.
6. Londhe PU, Rohom AB, Fernandes R, Kothari DC, Chaure NB. Development of superstrate $CuInGaSe_2$ thin film solar cells with low-cost electrochemical route from nonaqueous bath. ACS Sustain Chem& Eng. 2018;6(4):4987-95.
7. Xiaofeng LI, Yasushi W, Mao JW. Research situation and economic value of indium deposits. Miner Depos. 2007;26(4):475-80.
8. Hall SR, Stewart JM. The crystal structure refinement of chalcopyrite, $CuFeS_2$. Acta Crystallogr B. 2010;29(3):579-85.
9. Lyubutin IS, Lin CR, Starchikov SS, Siao YJ, Shaikh MO, Funtov KO, et al. Synthesis, structural and magnetic properties of self-organized single-crystalline nanobricks of chalcopyrite $CuFeS_2$. Acta Mater. 2013;61(11):3956-62.
10. Sil S, Dey A, Halder S, Datta J, Ray PP. Possibility to use hydrothermally synthesized $CuFeS_2$ nanocomposite as an acceptor in hybrid solar cell. J Mater Eng Perform. 2018;27(6):2649-54.
11. Bastola E, Bhandari KP, Subedi I, Podraza NJ, Ellingson RJ. Structural, optical, and hole transport properties of earth-abundant chalcopyrite ($CuFeS_2$) nanocrystals. MRS Commun. 2018;8(3):970-8.
12. Ding Y, Wang Y, Ni J, Shi L, Shi S, Tang W. First principles study of structural, vibrational and electronic properties of graphene-like MX_2 (M=Mo, Nb, W, Ta; X=S, Se, Te) monolayers. Physica B. 2011;406(11):2254-60.
13. Sopian K, Cheow SL, Zaidi SH. An overview of crystalline silicon solar cell technology: past, present, and future. AIP Conf Proc. 2017;1877:020004.
14. Wang Y, Lv S, Li Z. Review on incorporation of alkali elements and their effects in Cu(In,Ga)Se_2 solar cells. J Mater Sci Technol. 2022;96:179-89.
15. Dutkova E, Bujňáková Z, Kováč J, Škorvánek I, Sayagués MJ, Zorkovská A, et al. Mechanochemical synthesis, structural, magnetic, optical and electrooptical properties of CuFeS2 nanoparticles. Adv Powder Technol. 2018;29(8):1820-6.
16. Barkat L, Hamdadou N, Morsli M, Khelil A, Bernède JC. Growth and characterization of $CuFeS_2$ thin films. J Cryst Growth. 2006;297(2):426-31.
17. Takaki H, Kobayashi K, Shimono M, Kobayashi N, Hirose K, Tsujii N, et al. First-principles calculations of Seebeck coefficients in a magnetic semiconductor $CuFeS_2$. Appl Phys Lett. 2017;110(7):072107.
18. Delgado JM, Delgado G, Quintero M, Woolley JC. The crystal structure of copper iron selenide, $CuFeSe_2$. Mater Res Bull. 1992;27(3):367-73.
19. Berthebaud D, Lebedev OI, Maignan A. Thermoelectric properties of n-type cobalt doped chalcopyrite $Cu_{1x}Co_xFeS_2$ and p-type eskebornite $CuFeSe_2$. J Materiomics. 2015;1(1):68-74.
20. Urban DF, Ambacher O, Elssser C. First-principles calculation of electroacoustic properties of wurtzite (Al,Sc)N. Phys Rev B. 2021;103:115204.
21. Hou Q, Xi D, Li W, Jia X, Xu Z. First-principles research on the optical and electrical properties and mechanisms of In-doped ZnO. Physica B. 2018;537:258-66.
22. Wang Y, Ohishi Y, Kurosaki K, Muta H. A first-principles theoretical study on the potential thermoelectric properties of MgH_2 and CaH_2. Mater Res Express. 2019;6(5):055510.
23. Toprek D, Koteski V. Ab initio calculations of the structure, energetics and stability of AunTi (n = 1–32) clusters. Comput Theor Chem. 2016;1081:9-17.
24. Barhoumi M, Sfina N, Said M. Bandgap energy and dielectric function of GaOBr monolayer using density functional theory and beyond. Solid State Commun. 2021;329:114261.
25. Barth J, Johnson R, Cardona M, Fuchs D, Bradshaw AM. Dielectric function of between 10 and 35 eV. Phys Rev B Condens Matter. 1990;41(5):3291-4.